

Role of Eta-carbide Precipitation's in the Wear Resistance Improvements of Fe-12-Cr-Mo-V-1.4C Tool Steel by Cryogenic Treatment

Meng, Fanju, et al, Role of Eta-Carbide Precipitations in the Wear Resistance Improvements of Fe-12Cr-MoV-1.4C Tool Steel by Cryogenic Treatment, ISIJ International, Vol 34 (1994) No. 20 pp 205-210.

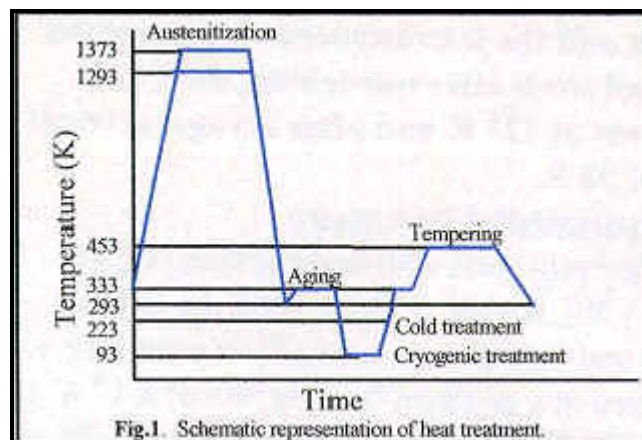
The wear resistance of an Fe-12.2wt%Cr-0.84wt%Mo-0.43wt%V-1.44wt%C alloy tool steel after cold treatment at 223K (-60f) and after cryogenic treatment at 93K (-292f) has been investigated. The wear resistance of steels after cryogenic treatment is superior to that after cold treatment. The effects of cryogenic treatment on the microstructure were also studied by means of X-ray diffraction and transmission electron microscopy methods. Unlike cold treatment, cryogenic treatment improves the preferential precipitation of fine n-carbides instead of e-carbides. These fine carbide particles enhance the strength and toughness of the martensite matrix and then increase the wear resistance. The formation mechanism of fine n-carbide is discussed.

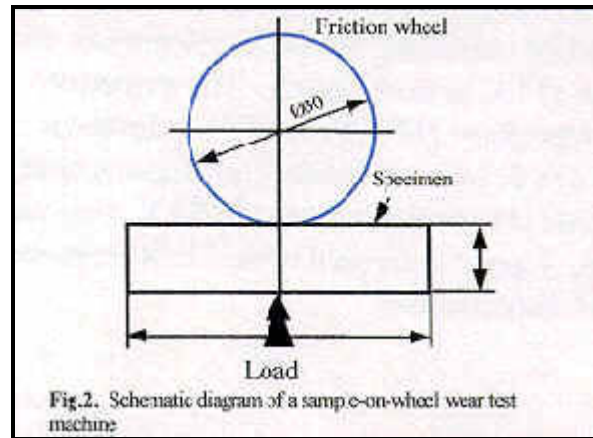
Although a lot of works about tempering behavior have been done, a complete and satisfactory understanding of the mechanisms of the structural changes involved has not yet been obtained. The 0-th stage, i.e., prior to carbide precipitation, and the first stage were of interest in the last decades. However, not so much attention has been paid to studying the effects of cryogenic treatments on the carbide precipitation in martensite during tempering.

The aims of the present study, therefore, are to investigate metallurgically the wear resistance and the microstructure of tempered alloy tool steels after quenching, after cold treatment at 223K and after cryogenic treatment at 93K.

2. Experimental procedure

Alloy tool steel with composition (wt%), 1.44C, 0.3Si, 0.4Mn, 12.2Cr, 0.84Mo, 0.43V, 0.022P, and 0.008S was used. Heat treatment was performed at a constant heating rate of 0.17K/s up to 1073K in a vacuum furnace at 4×10^{-3} Pa, then up to austenitizing temperature of 1293K or 1373K with a nitrogen atmosphere at 20 Pa, followed by quenching to room temperature and aging at 333K to avoid crack. The martensite start temperature (M_s) of this alloy is approximately 373K. Cold treatment at 223K and cryogenic treatment at 93K were carried out. Figure 1 shows a typical heat treatment cycle of experiments.



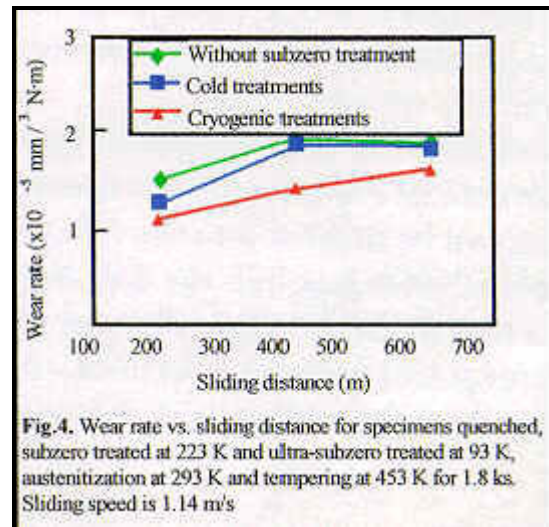
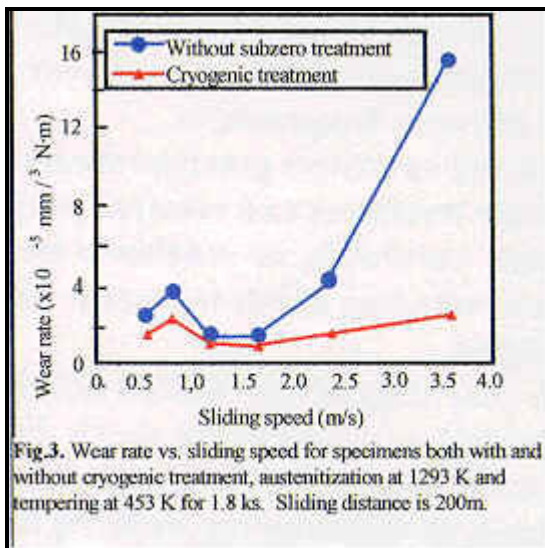


The specimens for the wear resistance with a size 25 x 50 x 10mm were ground and polished mechanically after tempering at 453K for 1.8Ks. A schematic diagram of a sample-on-wheel wear test machine is shown in fig. 2. A friction wheel, which has the same chemical composition as the specimens, was quenched and tempered with a hardness HV 780. No lubrication was used. The friction wheel rotated at a peripheral speed from .05 to 3.62m/s, the sliding distance was from 200 to 600m and the applied load was 21N. The wear rate, $W_s = Bb - 3/8rPL$, was calculated, where B is the thickness of the wheel, b is width of wear, r is the radius of the wheel, P is the applied load, and L is the sliding distance. The volume fraction of retained austenite was determined by X-ray phase analysis at room temperature. Peaks (211) of martensite and peaks (311) of the retained were employed. The thin sheets of approximately 100um in thickness for the observation of transmission electron microscopy (TEM) were austenitized and quenched by the same condition as mentioned above. The pressure of nitrogen atmosphere at 20Pa was controlled in order to avoid decarburization due to oxidation and/or evaporation during heat treatment. According to chemical analysis, the carbon content of the heat-treated sheets has been confirmed to be unchanged. Tempering was carried out at 453K for 600s after cold treatment and cryogenic treatment. The Theta 3mm discs were punched and jet-polished to perforation using an electrolyte of 10% HClO₄ and 90% CH₃ COOH at 283K.

3. Results

3.1 Wear Resistance

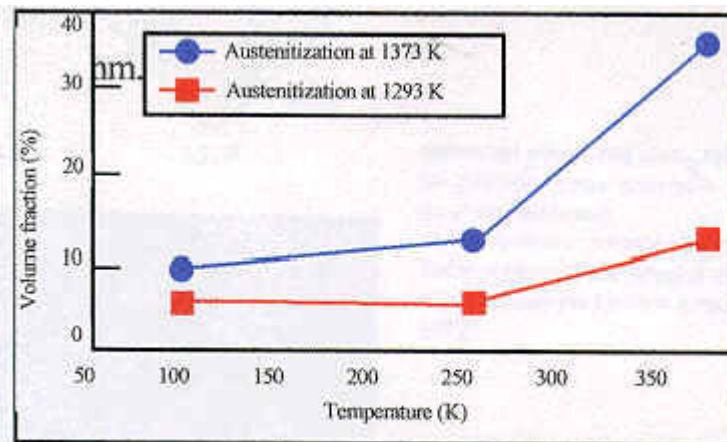
The Variation of the wear rate with sliding speeds is shown in Fig. 3 for specimens austenitized at 1293K, quenched and ultra-subzero treated at 93K. Finally tempering was carried out at 453K for 1.8Ks. The wear rate of specimens after cryogenic treatment is smaller than that of as-quenched specimens (without any subzero treatment) for whole sliding speeds. Furthermore, it decreases dramatically at high sliding speed. The cryogenic treatment results show 110 to 600% improvements. The wear rate shows a minimum at the sliding speed of 1.14 and 1.63m/s for specimens without and with cryogenic treatment, respectively.



In Fig. 4, the variation of the wear rate with sliding distance is shown for specimens quenched, subzero treated at 223K and ultra-subzero treated at 93K. The wear rate as of quenched specimens is larger than that of specimens after cold treatment and cryogenic treatment at sliding distance of 200m. At sliding distance of 400 and 600m, the specimens after cold treatment have almost the same wear rate as quenched specimens. However, the specimens after cryogenic treatment have a smaller wear rate than as quenched specimens and specimens after cold treatment for any sliding distance.

3.2 X-Ray Diffraction Analysis

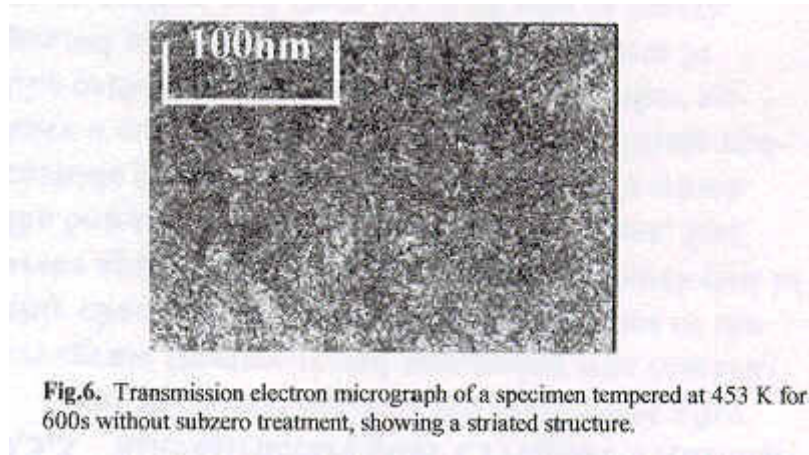
The volume fraction of retained austenite is plotted against the subzero treatment temperature in Fig. 5 for specimens austenitized at 1293K and 1373K. The volume fraction of retained austenite is 12% for as quenched specimens after austenitization at a 1293K and approximately 6% for specimens after cold and cryogenic treatment. However, it decreases with treating temperature going down for specimens austenitized as 1373K. Cold treatments reduce the volume fraction of retained austenite drastically. Nevertheless, cryogenic treatment reduces it slightly relative to cold treatment.



3.3 Structure Observation of TEM

3.3.1 As quenched and tempered structure

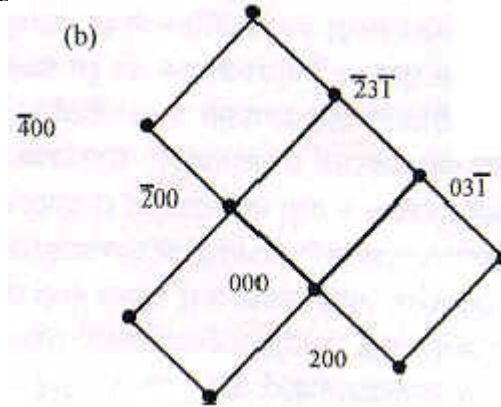
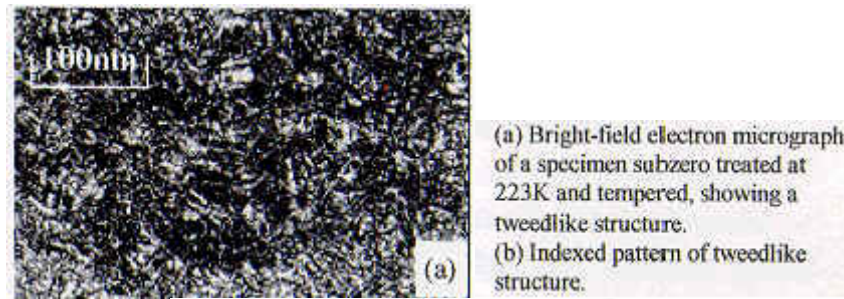
The microstructure of as quenched specimens consists of mainly fine twinned martensite and retained austenite, the spacing between twins being a few tens nm.



The bright field of Fig. 6 shows the microstructure of specimens quenched and tempered at 453K for 600s. The structure is mainly constructed with martensite and retained austenite. In the martensitic regions, many plates are internally twinned and some of the twins are extremely fine. The spacing between these twins being a few tens nm. On close examination, the twinned martensite shows coarse striated structure, which has been interpreted as the modulated structure produced by the spinodal decomposition, i.e., two variants of the carbon-rich regions. But there is a great difference from the results of Taylor and others. Only one set of fine parallel line contrasts was seen in the bright field image. The fine striations were spaced out about 1nm apart on average.

3.3.2 Microstructure after Cold Treatment

Fig. 7(a) shows the bright field image of specimens subzero treated at 223K and then tempered. Course tweedlike structure corresponding to two orientation variants was present. This fine scale modulated structure has a wavelength of about 5nm. However, carbide cannot be observed in the modulated microstructure. Fig. 7(b) is the selected area of deffraction pattern and the indexed pattern respectively, which consists of a (013) martensite zone. Inspection of deffraction pattern revealed streaking due to spinodal decomposition during the 0-th stage of tempering.



3.3.3 Microstructure after Cryogenic Treatment

The microstructure of the martensite after cryogenic treatment and tempering was remarkably changed, shown in Fig. 8(a). In most of the areas appeared fine carbide particles developed in the boundary of twins. In different areas, fine carbide particles appeared at the points, which have a considerable diffusing density. Some rod like carbide particles parallel to each other appeared and varied in size from 5 to 10nm in cross-section and from 20 to 40nm in length.

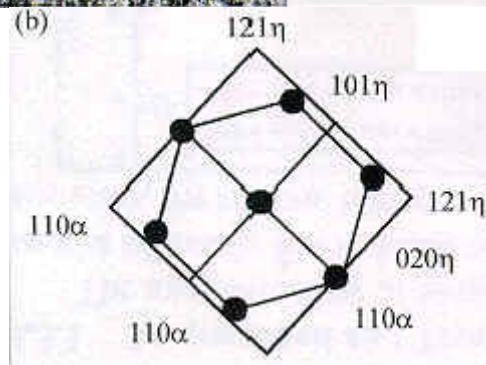
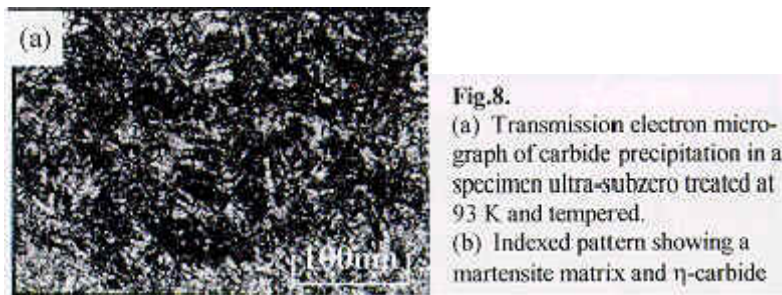


Fig.8.
 (a) Transmission electron micrograph of carbide precipitation in a specimen ultra-subzero treated at 93 K and tempered.
 (b) Indexed pattern showing a martensite matrix and η -carbide

Fig. 8(b) is the selected area diffraction pattern and the indexed pattern, respectively. The diffraction pattern consists of a (111) martensite zone and a (101) n-carbide zone. It was seen that the (011) martensite plane is parallel to the (010) n-carbide plane, the (111) martensite direction is parallel to the (101) n-carbide direction.

From this pattern, it could be confirmed that the orientation relationship between martensite (x) and n-carbide is the Hirotsu and Nagakura relationship, as indicated below. (011) X // (010) n; (111) X // (101) n. Jack identified transition carbide, which forms during tempering between 350K and 430K as hexagonal e-carbide. Table 1 compares the difference associated with the indexing of the carbide diffraction pattern according to published values of (d-hk1) for n-carbides and e-carbides. Although there is a close similarity between the structure of n and e-carbide, it is clear that the precipitated phase is n-carbide rather than e-carbide.

4. Discussion

4.1 Relationship between Wear Resistance and Retained Austenite

From Fig. 5, the specimens austenitized at 1293K, subzero treated at 223K and ultra-subzero treated at 93K have almost the same volume fraction of retained austenite. However, the specimens after cryogenic treatment show wear resistance improvement considerably, as shown in Fig. 4. Although the specimens after cold treatment have a smaller volume fraction of the retained austenite than that of the as quenched ones, both have almost the same wear rate at sliding distances 400 and 600m. It is accepted that a major factor contributing to wear resistance improvement through subzero or ultra-subzero treatment is the removal of retained austenite and the formation of homogeneous martensitic structure although the hardness is hardly changed. According to the scanning electron microscopy observation of the worm surface of hardened carbon tool steel tempered at temperatures lower than 573K by Huet al., the predominant wear mechanisms were ploughing fatigue, fracture and delamination. In this case, the wear rate may be controlled by crack nucleation and propagation beneath the surface, which is related to the strength and toughness of the materials. Retained austenite may prevent crack propagation either by changing the growth direction of an advancing crack or by great energy absorption. It is suggested that cryogenic treatment makes a contribution to wear resistance due to fine n-carbides precipitation rather than the removal of retained austenite.

4.2 Mechanism of n-carbide Precipitation

A model of the bct-orthorhombic system transformation is proposed. It is known that the lattice deformation of martensite results from cryogenic treatment.

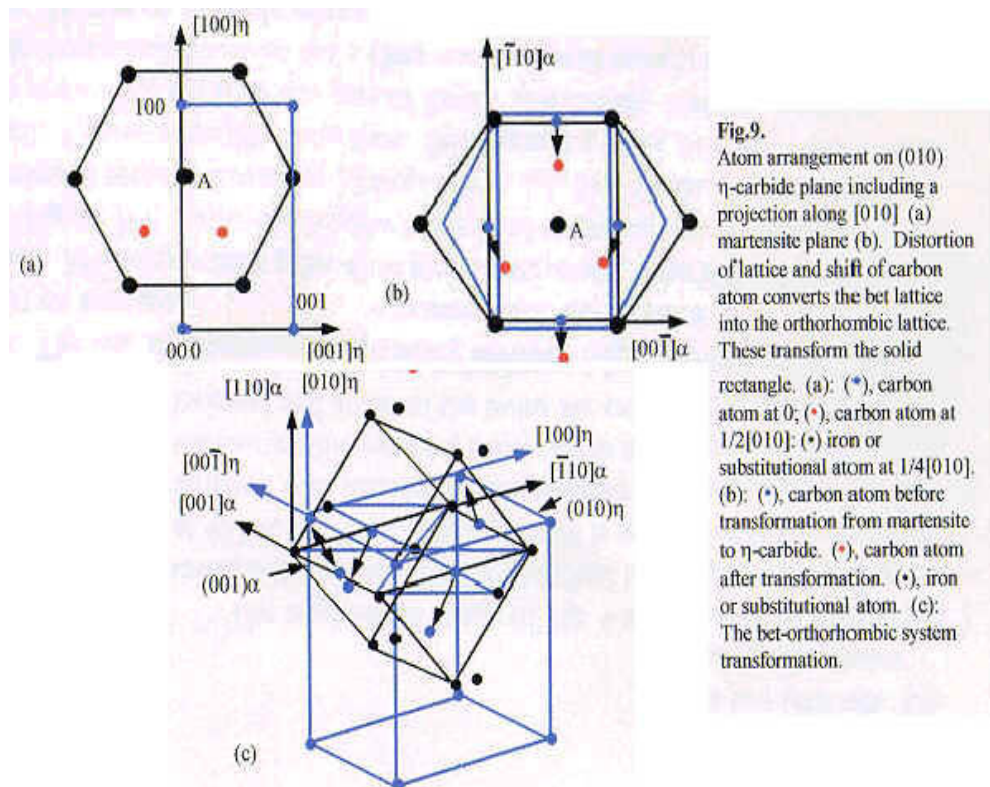


Fig. 9(a) and (b) represent the relationship between (010) n-carbide plane and (110) martensite plane. This existence of the lattice correspondence between two phases implies that (010) n-carbide plane is derived from (110), (110) and (001) martensite directions respectively. In the n-carbide structure, carbon atoms are in the octahedral interstices and iron or substitutional atoms in n-carbide and martensite is AB(n), AB(x), BC(n), BC(x). The lattice deformation is supposed to convert the parent bct lattice into an orthorhombic n-carbide lattice through the readjustment of iron or substitutional atoms due to contraction along (110) and (110) martensite direction of expansion along (001) martensite direction. Correspondingly, a slight shift of carbon atoms is required on (110) martensite planes in order to achieve carbon atoms stacking of n-carbide. This can be present as follows in bct lattice, carbon atoms at $(1/2, 1/2, 0)$ and $(1/2, 1/2, 1)$ positions in (110) martensite plane shift $a/12(15)$, which may be explained $a/6(110)+a/4(110)$, and ones at $(0, 1, 1/2)$ and $(1, 0, 1/2)$ position shift $a/12(510)$, i.e. $a/6(110)+a/4(110)$, where a means the lattice parameter of martensite. Furthermore, before contraction and expansion, a $a/6(110)$ shuffling of iron or substitutional atoms on alternate (110) martensite plane is necessary to meet the needs of stocking described n-carbide structure. Alternatively, iron or substitutional atoms and carbon atoms in the other (110) martensite planes also change correspondingly as indicated above. Fig. 9(c) shows the bct-orthorhombic system transformation. The plain circle indicate iron or substitutional atoms, the double circles indicate iron or substitutional atoms which belong to two unit cells and the solid circle indicate carbon atoms. The shuffling direction of atoms is shown by an arrow. It is suggested by TEM observation and crystallographic analysis of carbide that carbide nucleates heterogeneously along the carbon-rich bands which develops during the spinodal decomposition of martensite. It is well known that precipitation of fine n-carbide enhances strength and toughness of martensite matrix, and further increases wear resistance.

5. Conclusion

(1) Cryogenic Treatment increases wear resistance dramatically, especially at high sliding speed. The specimens after cryogenic treatment show a minimum of wear rate.

(2) Unlike cold treatment, cryogenic treatment promotes preferential precipitation of fine n-carbides.

(3) The formation mechanism of n-carbides is supposed to be as follows: iron or substitutional atoms expand and contract, and carbon atoms shift slightly due to lattice deformation as a result of cryogenic treatment.

(4) The mechanism that cryogenic treatment contributes to wear resistance is through the precipitation of fine n-carbide, which enhances strength, and toughness of martensite matrix, rather than the removal of the retained austenite.